applied sciences

MDPI

Article

Study on Elevator Recognition Techniques for Upper-Limb-Disabled Wheelchair Users

Daewe Kim, Su-Hong Eom and Eung-Hyuk Lee *

Department of Electronics Engineering, Tech University of Korea, Gyeonggi 15073, Republic of Korea; ihlab.dwkim@gmail.com (D.K.); sheom@tukorea.ac.kr (S.-H.E.)
* Correspondence: ehlee@tukorea.ac.kr

Abstract: This study proposes a LiDAR-sensor-based elevator recognition technique to prevent collisions caused by poor operation and the cognitive decline of wheelchair users with upper limb disabilities. Existing elevator recognition studies show high performance for elevator door recognition, but this can only be recognized at a position where the elevator can be viewed directly due to the angle of view range of the sensor. This is not appropriate for wheelchair users who are inexperienced in operation because alignment must be performed directly based on the elevator. Therefore, this study presents a LiDAR-sensor-based elevator recognition technique that can detect elevators from the side to the position and at an angle to the front in order to solve this problem. In addition, this study proposes a technique for recognizing elevator gates finished with low- and high-reflective materials in order to enable recognition in various elevator environments. In order to quantitatively verify the elevator recognition technique proposed in this study, experiments were conducted in an elevator environment consisting of low and high reflections. The results of the experiments confirmed that there was no problem in applying the wheelchair active driving technique.

Keywords: electric wheelchair; upper limb disabled; collision; inadequate operation; safety; LiDAR; elevator; elevator detection; reflectivity

check for updates

Citation: Kim, D.; Eom, S.-H.; Lee, E.-H. Study on Elevator Recognition Techniques for Upper-Limb-Disabled Wheelchair Users. *Appl. Sci.* **2023**, *13*, 12182. https://doi.org/10.3390/app132212182

Academic Editor: Antonio Bandera

Received: 24 October 2023
Revised: 6 November 2023
Accepted: 7 November 2023
Published: 9 November 2023

Copyright: © 2023 by the authors. Licensee MDPI, Basel, Switzerland. This article is an open access article distributed under the terms and conditions of the Creative Commons Attribution (CC BY) license (https://creativecommons.org/licenses/by/4.0/).

1. Introduction

According to the World Health Organization (WHO), there were about 1.3 billion disabled people in the world as of 2022, accounting for about 16% of the total population, including people who have difficulty walking and require the use of a wheelchair [1,2]. There are two main types of wheelchairs: manual wheelchairs that move by pushing the pushrim directly by hand, and electric wheelchairs that enable movement through use of a controlling joystick [3,4]. Users of manual wheelchairs may experience lack of endurance in arm muscle strength or difficulty driving on ramps during long-distance driving. On the other hand, electric wheelchairs are suitable for users who have difficulty driving due to lack of arm strength and endurance because they enable movement by control of a controller joystick using a small force [4,5].

However, according to an in-depth survey of patients with emergency room injuries caused by electric wheelchair accidents, 93.6% of 407 people surveyed experienced collisions [6]. The main cause of collision accidents with obstacles was the user's inexperience in manipulation and cognitive decline. The biggest reason for accidents caused by wheelchair manipulation errors or inadequate operations is the failure to respond appropriately in unexpected situations. Therefore, among wheelchair users, those who suffer from severe disabilities are exposed to the risk of accidents resulting from upper limb physical function decline. The reason is that the most severely disabled people with impaired upper limb physical function have symptoms such as shaking, stiffness, and weakness of the arms or hands, and these symptoms can cause problems in wheelchair manipulation [7].

In the past, research has focused on improving the operation of electric wheelchairs for people who have difficulty with operating joysticks, but with the development of

autonomous driving technology, researchers are trying to apply this technology to electric wheelchairs. However, although autonomous driving technology is effective where there is a structured map, there is still a problem of safety in areas where the nature of the space changes, such as moving between floors and riding an elevator. Therefore, in this paper, we propose a technique for elevator door recognition and doorway width estimation for wheelchair entry in an autonomous wheelchair system to ensure that a wheelchair can safely enter the elevator.

Recent studies on elevator recognition include those examining depth-camera-based elevator recognition and strong elevator door recognition using an LRF (laser range finder) and cameras [8–15].

A study on depth-camera-based elevator recognition suggested a method of finding the exact location of the door using forward-oriented, three-dimensional distance data and particle filters for incorrect initial location of the elevator door. The experiment findings suggested that the average position error and angle error between the actual door position and the recognized position were 8 cm and 2° or less, respectively [8].

In the case of elevator recognition studies using an LRF and cameras, in one study, a camera-image-based door verification process was added to the existing method, which used an LRF only, producing a high elevator door recognition rate of 96.7% when looking at the elevator from the front [11].

However, existing elevator recognition studies only consider a position where the elevator can be viewed directly from the front due to the angle of view range of the sensor. This requires driving and aligning to a position where the user directly faces the front to perform elevator recognition. However, it is not appropriate for an inexperienced wheelchair user to drive from the location of the call switch to the location and correct angle for boarding the elevator.

Electric wheelchairs are divided into rear-wheel-, front-wheel-, and mid-wheel-drive types, with the center of rotation located at the rear, front, and middle, respectively. The front-wheel- and mid-wheel-drive types exhibit no difficulties in a narrow environment due to their narrow turning radius [16]. However, due to the nature of the platform, driving is unstable on non-flat ground because of low shock absorption, making it unsuitable for outdoor use [16,17]. On the other hand, the rear-wheel-drive type does not comply with the restrictions of the application environment because it allows relatively stable driving even on non-flat ground due to its high shock absorption power [16,17]. However, unlike the front-wheel- and mid-wheel-drive types, the rear-wheel-drive type can cause collisions during the alignment to prepare for elevator boarding due to the wide turning radius and relatively difficult manipulation in front of the wheelchair. In addition, wheelchair users are located at an angle to the front or side with the elevator when pressing the elevator call switch, so the driving process for the alignment varies depending on the situation.

Therefore, this study presents a LiDAR-sensor-based elevator recognition technique that can detect the elevator from the position and angle in front of the rear-wheel-drive wheelchair user considering boarding of the elevator in order to solve this problem.

Existing elevator recognition studies used LiDAR sensors that measure fast and accurate distance values to solve the inconvenience of maintenance and repair, which is a limitation of elevator recognition using Marker [8–11]. Since LiDAR sensors measure distances using light sources, the reliability of the measured distance data is determined by the type of surface material measured [14]. Various finishing materials for elevators are used, and elevators made of steel or of mirror-type stainless steel with high surface reflectivity should be additionally considered when performing elevator recognition based on LiDAR sensors.

However, sensors that measure distances using light sources, such as LiDAR, show good performance with general materials with low reflectivity, but high-reflective materials with high reflectivity result in low recognition performance due to the diffused reflection of light. When scanning an elevator door finished with a low-reflective material with low surface reflectance, the shape of the elevator is clearly shown in the LiDAR raw data

collected. For this reason, recognition techniques using the regularity of data are possible. However, in the case of elevators made of high-reflective materials with high surface reflectance, recognition techniques depending on regularity are impossible to use due to a high level of measurement errors in the collected data [18].

Therefore, this study proposes a technique for recognizing elevator doors finished with low- and high-reflective materials to enable elevator recognition in various elevator environments. The purpose of the proposed method is not to determine the existence of an elevator gate in the system using the vision sensor and AI technology described above, but to calculate the effective distance and coordinates for electric wheelchair entry according to the elevator structure. Therefore, the technique proposed in this paper uses LiDAR sensors based on distance information. However, since the LiDAR approach involves a sensor that uses a light source, it is necessary to take measurements according to the elevator surface material; thus, this method estimates the width and coordinates of the elevator door based on the structural features of the elevator boarding gate.

The proposed recognition technique recognizes the elevator boarding gate based on the threshold value in points collected from LiDAR containing information on the boarding gate, using the lines created by the ABD (adaptive breakpoint detector) segmentation algorithm that actively responds according to the LiDAR's measurement distance and the split-and-merge-based IEPF (iterative end point fit) line segment extraction algorithm that can more clearly detect the boundary of the structure.

In order to quantitatively verify the elevator recognition technique proposed in this study, experiments were conducted in an elevator environment consisting of low and high reflections. The recognition rate and precision for the low-reflection finish were 80% and 6.11 cm, respectively, and the recognition rate and precision for the high-reflection finish were 73.3% and 5.81 cm, respectively.

This paper proposes a method for elevator boarding gate recognition and width estimation. In the Materials and Methods section, the theoretical background of the algorithm to shape the elevator structure based on the raw data of LiDAR and the proposed elevator recognition technique are presented. In the Results and the Conclusions sections, an evaluation contrasting the recognition and width estimation of the elevator boarding gate with low-reflective and high-reflective finished materials is reported for the quantitative verification of the proposed theory.

2. Materials and Methods

2.1. Elevator Analysis

Since the elevator recognition is performed based on LiDAR sensors in this study, the structure of the elevator should be considered. The elevator structure consists of three main types: an elevator door for passengers to get on and off, a door frame surrounding the gate to the elevator, and a car that is a part of the elevator carrying the passengers or cargo, as shown in Figure 1 [19]. The elevator structure that can be measured by LiDAR when the door of the elevator is closed includes the elevator door and the door frame, and these two factors are used to set the recognition conditions for the elevator gate.

As the elevator recognition is conducted based on LiDAR sensors whose measurement data is affected by the materials employed, the material of the elevator should be considered. Figure 2 shows the results when the elevator is finished with low- and high-reflective materials and is scanned at the central location of the boarding gate. Point groups collected from the LiDAR sensors are referred to as the point-cloud. The shape of the elevator in the point-cloud is relatively clear for low-reflective materials, while the shape of the elevator in the point-cloud cannot be identified with high-reflective materials with high surface reflectance.

Using a light-source-based LiDAR sensor, it is found that scanning the elevator door and the door frame at the center of the gate of the high-reflective elevator generates noise due to large reflection angles and high surface reflectance in the door frame. Since the results of the noise forms generated depending on the location of the LiDAR sensor are different, there is a limit to the ability to apply the elevator form as a recognition condition as for a low-reflection

elevator. To solve this problem, the recognition conditions should be set based on the door and adjacent wall of the high-reflective elevator with relatively low noise.

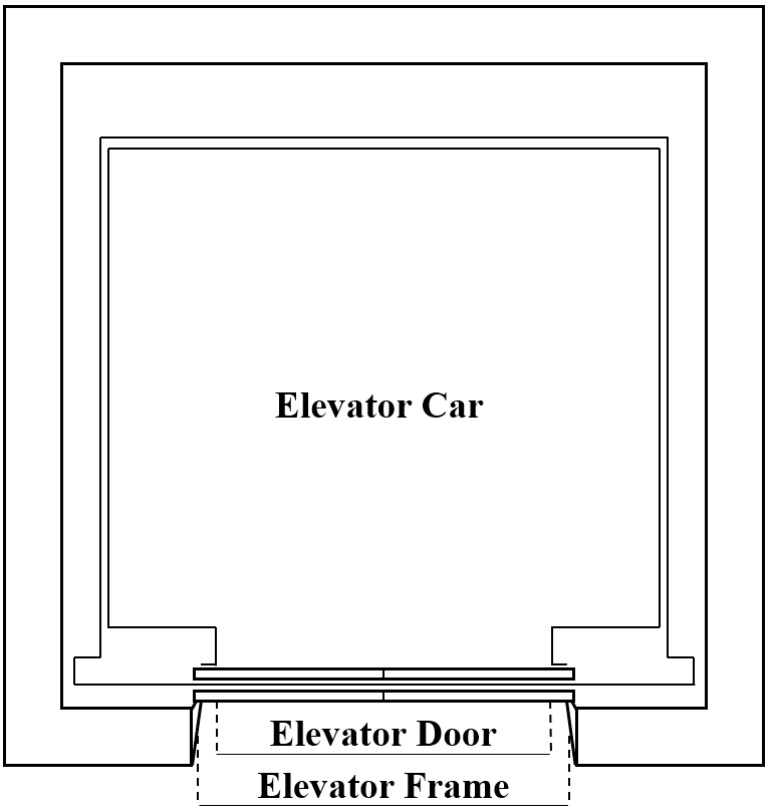


Figure 1. Elevator floor plan.



(**a**) LiDAR data of low-reflection elevator (**b**) LiDAR data of high-reflection elevator

Figure 2. Low- and high-reflection elevator.

In terms of the structural characteristics of the elevator, the door of the elevator is opened and closed from the center and the side, which requires a space for storing the door. In order to secure a space where the elevator door is stored, an elevator wall structure is needed.

Therefore, this study proposes a recognition technique based on the elevator door and wall structure to overcome the limitations of direct recognition according to the reflectance of the elevator door finishing material.

2.2. LiDAR-Sensor-Based Gate Structure Shape Recognition Method

This study proposes a LiDAR-sensor-based elevator gate recognition algorithm for elevator gate recognition. Although the elevator recognition algorithm sets elevator gate recognition conditions based on the door and door frame, it is impossible to recognize the elevator if it is finished with high-reflective materials and has high surface reflectance based on its shape due to the nature of the LiDAR sensors because of significant noise in the door frame. Therefore, in order to recognize an elevator gate with high-reflective materials, high-reflective elevator recognition conditions are set based on the adjacent walls and elevator doors with small surface reflectance.

The elevator gate recognition technique detects the elevator at the position and angle of the front from the side and accurately detects the coordinates of the elevator door frame. Before applying the elevator recognition technique, filtering is performed to remove noise in the point-cloud collected from the LiDAR sensor in advance to improve the recognition rate. Then, the elevator recognition is implemented using the characteristic points of the elevator structure based on the lines created by the segmentation and line segment extraction algorithm in the point-cloud where the noise is removed.

2.2.1. Filtering to Improve Elevator Recognition Rate

The width of the elevator gate is narrow, so to pass safely considering the width of the electric wheelchair, accurate coordinates of the elevator door frame must be detected for safe driving [14]. Therefore, in order to accurately detect the coordinates of the elevator, a low-pass filter (LPF) is applied to remove noise from the raw data collected from LiDAR.

An LPF is used to remove a high frequency signal from the data components in the point-cloud generated by the LiDAR sensor. The relational equation is shown in Equation (1):

$$\overline{x_k} = W\overline{x_{k-1}} + (1 - W)x_k\ ,\ \ (0 < W < 1) \tag{1}$$

This study proposes an algorithm to recognize the shape of the elevator in the collected point-cloud. However, if there is an object similar to an elevator within the point-cloud, there is the possibility of misrecognition. In addition, when measuring high-reflective materials, these can be measured differently from actual distance information due to their high surface reflectance, which is an obstacle to the recognition algorithm process. Therefore, it is necessary to apply a technique of masking the data based on the distance value measured from LiDAR to prevent misrecognition of elevator-like forms and unnecessary noise. The masking technique is a method of removing unnecessary data by treating it as null when the measured distance value is greater than the value of $threshold_{max}$ or less than the set value of $threshold_{min}$, as shown in Equation (2). The threshold value is set in consideration of the position where the wheelchair user presses the elevator call switch.

$$x_n = null\ ,\ \ (x_n > threshold_{max}\ \ ||\ \ x_n < threshold_{min}) \tag{2}$$

2.2.2. Clustering and Line Segment Extraction Techniques for the Recognition of Gate Structure Shapes

In order to perform the elevator recognition technique, it is necessary to analyze point data in the point-cloud. This can be implemented though a segmentation process for extracting a set of points with information on the elevator gate, and a line segment extraction process to perform a test of the elevator gate recognition conditions for each set.

Segmentation is a data-processing technique that divides a given data set into several areas, and algorithms should be selected appropriately according to the acquisition environment and the purpose of clustering. Segmentation algorithms typically include K-means, DBSCAN (density-based spatial clustering of applications with noise), and ABD (adaptive breakpoint detector).

A general clustering method performs area division based on a threshold value in which the Euclidean distance between consecutive points is fixed [20]. However, since this method has the problem that it is not formed as a single cluster for areas with low point data density, points belonging to the elevator may not be formed as a single segment due to the position of the LiDAR sensor determined by wheelchair user manipulation.

Among the ways to improve the limitations of the general clustering methods, the K-means algorithm is a method of clustering the collected data into k clusters, which is simple and fast [21,22]. However, the number of clusters must be specified, which is not appropriate considering that the number of clusters created when scanning the elevator gate depends on the LiDAR location.

DBSCAN is a method of forming clusters based on the density of points collected by a density-based clustering algorithm, and it does not require a predefined number of clusters and can detect clusters of various shapes and densities [22–24]. However, the DBSCAN algorithm needs to set a fixed bandwidth for setting the criteria for clustering. This is not suitable because the number of clusters according to the elevator shape may be inappropriately generated according to the position of the wheelchair.

On the other hand, ABD performs clustering by adaptively responding to the threshold value that determines the criteria for segmentation according to the measurement distance of the LiDAR sensor. This does not require setting the number of clusters in advance, and clustering is carried out according to the measured distance. Thus, clustering according to the elevator shape is properly performed regardless of the location of the wheelchair.

Therefore, this study applied the ABD (adaptive breakpoint detector) segmentation algorithm that adaptively responds to the threshold value, which sets the segmentation standard, as shown in Figure 3, according to the measurement distance of the LiDAR sensor. The radius of the threshold circle can be obtained through Equation (3) and is the noise of the sensor device according to the measured distance value. Based on this, if the distance value $d_{eucliddistance}$ between the points p_{n-1} and p_n calculated through Equation (4) is greater than $D_{threshold}$, it is separated into a new cluster. The condition for separating into new clusters is shown in Equation (5).

$$D_{threshold} = |r_{n-1}(\sin\lambda / \sin(\lambda - Q)| + 3\sigma \tag{3}$$

$$d_{eucleddistance} = \sqrt{(x_n - x_{n-1})^2 + (y_n - y_{n-1})^2} \tag{4}$$

$$d_{eucleddistance} \geq D_{thresholdradius} \tag{5}$$

In order to recognize the elevator based on the clusters generated through the ABD clustering algorithm, information on the line segments representing the characteristics of each cluster must be obtained, which is performed through the line segment extraction technique.

According to V. Nguyen [25], the incremental algorithm is an algorithm that extracts new lines using information from previously extracted lines, which is fast and accurate. However, errors can be accumulated because they depend on the previous results, which are not suitable for use in noise-producing, high-reflective elevator environments. Although the RANSAC, HT (Hough transform), and EM (expectation maximization) algorithms have higher precision than other line segment extraction algorithms, the line segment extraction accuracy of doors and door frames for the elevator gate recognition is low. Accordingly,

they are not suitable for elevator recognition because there is a probability of misrecognition due to their low accuracy.

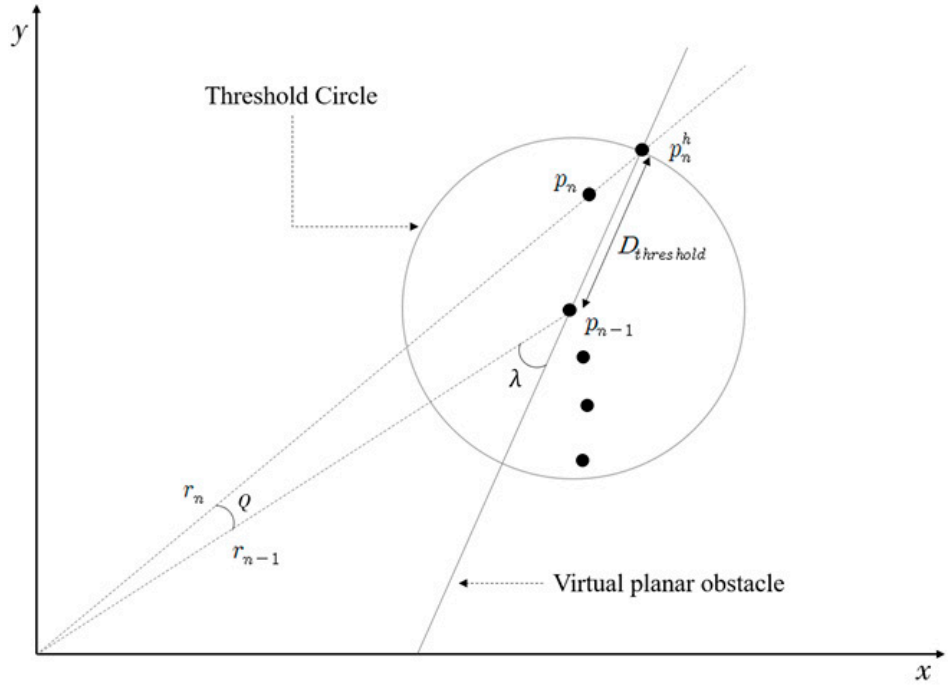


Figure 3. ABD clustering algorithm.

The split-and-merge algorithm showed relatively fast performance speed and high line segment extraction accuracy, and there was no accumulation of errors, which is a problem with the incremental approach. It also has high line segment extraction accuracy, unlike the RANSAC, HT, and EM algorithms. The IEPF (interactive end point fit) algorithm based on split-and-merge is suitable for use in structures such as elevator gates due to its high line segment extraction accuracy and excellent ability to accurately extract the end point of the line segment. For this reason, the IEPF line segment extraction algorithm was applied in this study [26,27].

Therefore, in this study, the IEPF line segment extraction algorithm was used as a method to extract the line segment of clusters with elevator information. The line segment extraction process of the IEPF algorithm repeats the split-and-merge process compared to $threshold_{thd}$, a factor that determines the split process based on the point where the distance between $breakpoint_{start}$, the starting point of each cluster, and the line L passing through $breakpoint_{end}$, the ending point, and points existing in other clusters meet, as shown in Figure 4.

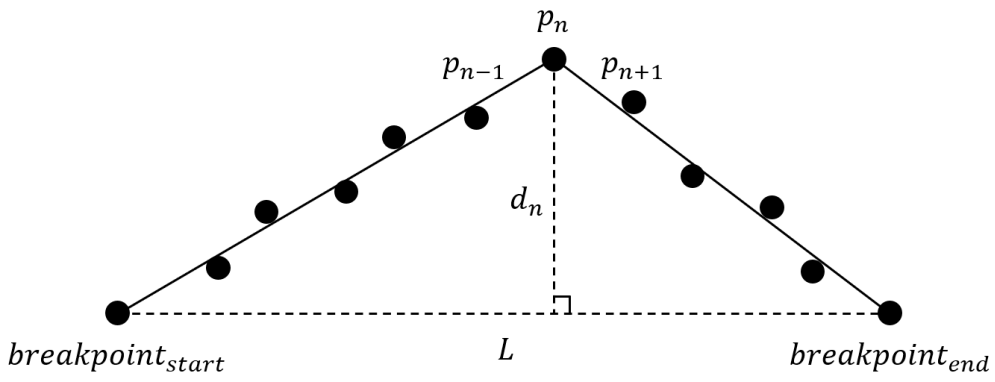


Figure 4. IEPF line extraction algorithm.

2.2.3. Elevator Feature Point-Based Recognition Method

In order to recognize the elevator, detection conditions should be set according to the characteristics of the elevator structure. This study presents a recognition algorithm using the characteristics of line segments generated through the IEPF line segment extraction algorithm. The elevator recognition technique determines whether or not the recognition technique is implemented by comparing the number of lines generated through the IEPF with the minimum number of lines that can represent the shape of the elevator, as shown in Figure 5. The elevator recognition technique first performs low-reflective elevator recognition, and if it is not detected, high-reflective elevator recognition is performed to determine whether the elevator is detected.

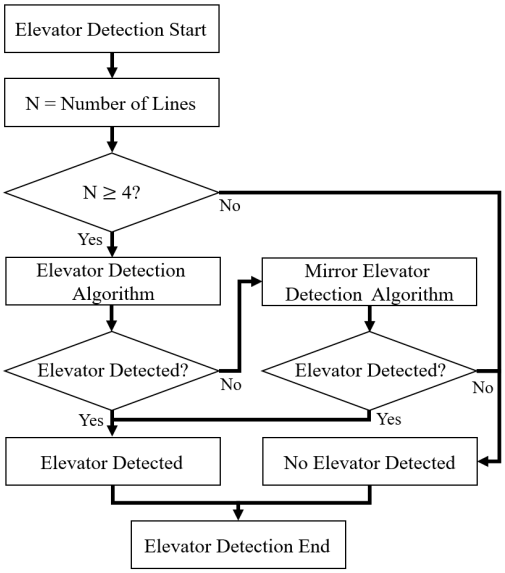


Figure 5. Elevator detection algorithm flowchart.

The point-cloud type containing elevator information is divided into two cases, depending on the location of the LiDAR sensor being scanned, as shown in Figure 6. CASE 1 of Figure 6 shows the case where the scan was performed at a position where the LiDAR sensor could detect the entire structure of the elevator, and CASE 2 shows the result of the scan at a position where the right side of the elevator was not detected. Therefore, in this study, the elevator feature detection conditions are examined based on the extracted line segments to recognize the two types of elevators determined by the location of the LiDAR sensor.

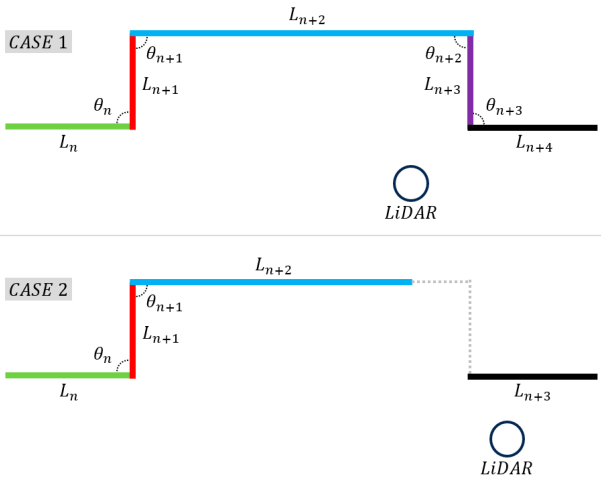


Figure 6. Elevator feature detection.

The test of the elevator feature detection conditions is based on the angle between the adjacent line segments, and the length of the line segment with the elevator door frame and door information; the algorithm for this is shown in Algorithm 1. The final condition of the elevator recognition algorithm process is based on the distance between the test points corresponding to the elevator door frame. In this study, an elevator recognition algorithm is carried out based on the minimum effective door width of 0.8 m for disabled elevators under the Korea Act on Guaranteeing Convenience Promotion of Elderly Pregnant Women with Disabilities for the elevator feature test [28].

Algorithm 1. Elevator Detection

Notation
s_n = start point of n^{th} line
e_n = end point of n^{th} line
θ_n = degree between adjacent line
θ_{thr} = threshold degree range
d_n = n^{th} line length
d_{fthr} = elevator frame threshold range
d_{dthr} = elevator door threshold range
l_s = straight line through points e_n, s_{n+1}
flag = elevator detection status

```
Detect (s_n, e_n, d_n, θ_n) {
for i from 1 to 4
    if θ_n is within the threshold degree:
        n = n + 1
        if i is 1 or 3:
            if d_n is within the d_fthr
            else return
        end if
        if i is 4:
            coordinates = (e_n, s_n+4)
            flag = true
            break
        end if
        ifd_n is within the d_dthr:
        else break
        end if
    else if i is 3:
        if an angle between l_n+2, l_s is within θ_thr
            if an angle between l_n+3, l_s is within θ_thr
            coordinates = (e_n, s_n+3)
            flag = true
end for
if flag is true
    if coordinates distance satisfy elevator width
        return coordinates
end if
}
```

Due to the nature of the LiDAR sensors, the point-cloud, which includes information on high-reflective elevators, is generated in a very irregular form due to high surface reflectance, making it difficult to use points that scan the elevator structures. According to W. Chen [29,30], disturbance observer-based control (DOBC) is a control methodology that estimates and compensates for disturbances in linear and nonlinear systems and has shown good performance in the presence of disturbances. However, this technique is suitable for smooth nonlinear disturbances and is not suitable for non-smooth noisy environments.

Therefore, in this study, a recognition technique using the adjacent wall of the elevator is performed as a means of recognizing the high-reflective elevator.

The method of using the adjacent wall of the elevator is based on the slope and distance information of the line segments collected through the line segment extraction algorithm, as shown in Figure 7. A mirror-type elevator feature condition test is conducted with a sequence of inspecting each line segment based on the gradient information and the end point of the reference line segment l_n.

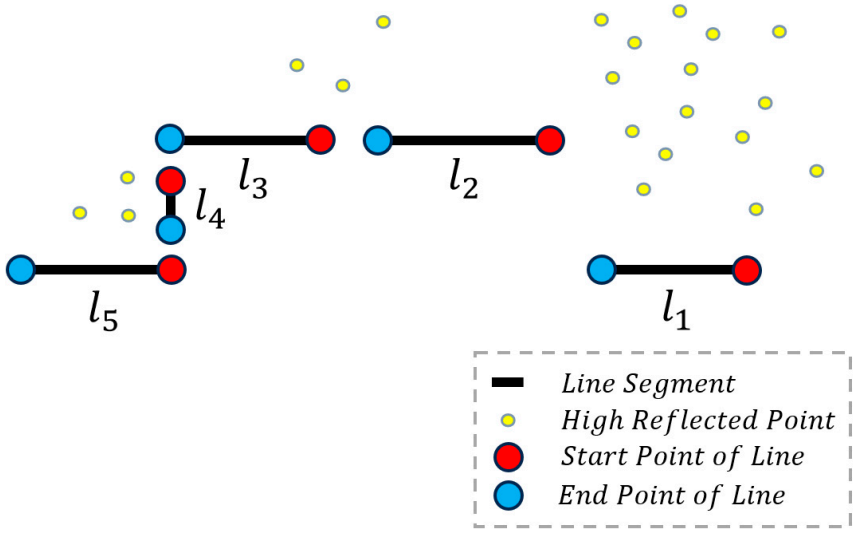


Figure 7. High-reflection elevator detection algorithm.

As shown in Equation (6), the first condition is presented in Equation (7) as a method to determine whether the slope value m_{n+k} of the line segment l_{n+k} to be tested has a value similar to the gradient value m_n of the baseline segment l_n.

The second condition is the process of calculating the distance between the start point of l_{n+k} and the end point of l_n by applying Equation (8) and determining whether the result value satisfies the minimum door width condition of the elevator, which is performed through Equation (9).

The last condition is to prevent the process of identifying l_3 in Figure 7 that satisfies the first and second conditions as the adjacent wall of the elevator, and through applying Equation (10), the slope value k of the line passing through the start point of l_{n+k} and the end point of l_n is obtained, and it is determined whether it has a value similar to the slope of l_n through Equation (11).

$$m_n = \frac{\Delta x_n}{\Delta y_n}, \quad m_{n+k} = \frac{\Delta x_{n+k}}{\Delta y_{n+k}} \tag{6}$$

$$m_n - \alpha \leq m_{n+k} \leq m_n + \alpha \tag{7}$$

$$d = \sqrt{(x_{n+k} - x'_n)^2 + (y_n - y'_n)^2} \tag{8}$$

$$d \geq d_{elevator\ minimum\ width} \tag{9}$$

$$d_{eucleddistance} = \frac{y_{n+k} - y'_n}{x_{n+k} - x'_n} \tag{10}$$

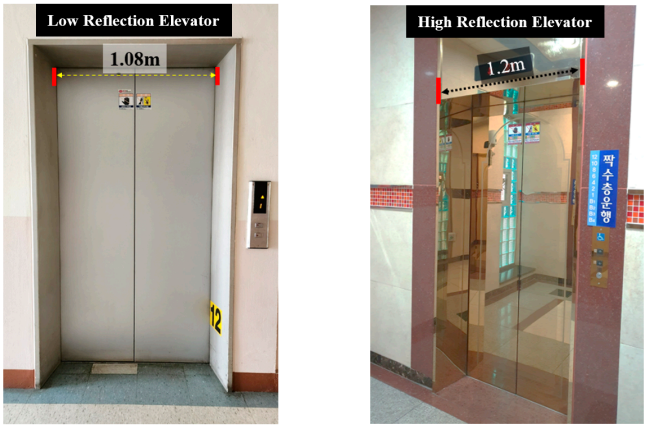
$$m_n - \alpha \leq k \leq m_n + \alpha \tag{11}$$

3. Results

3.1. Experimental Environment and H/W Configuration

3.1.1. Experimental Environment

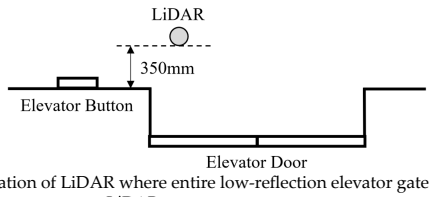
This study presents a technique for recognizing elevator gates instead of users in various elevator environments of wheelchair users with upper limb disabilities with symptoms such as tremors, stiffness, and weakness that can affect wheelchair manipulation. To verify the proposed technique, a recognition experiment was conducted in an elevator environment finished with a low-reflective material with a passage effective width of 1.08 m, and a high-reflective material with a passage effective width of 1.2 m, as shown in Figure 8. To quantify the elevator reflectance of the low- and high-reflective materials, the surface reflectance was measured through an ARM-216 reflectance meter, AMITARI, and 51.3% and 94.2% were identified for the low- and high-reflective material finishes, respectively.



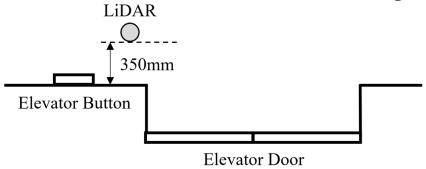
(**a**) Low-reflection elevator (**b**) High-reflection elevator

Figure 8. Low- and high-reflection elevator environment.

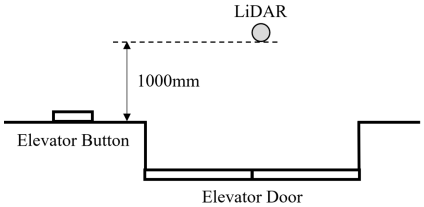
In the experiment for low-reflective elevator recognition, verification of the elevator gate recognition technique was conducted at a location where the entire elevator gate is detected through the LiDAR sensor and a location where one elevator door frame is not detected, as shown in Figure 9a and 9b, respectively.



(**a**) Location of LiDAR where entire low-reflection elevator gate is detected



(**b**) Location of LiDAR where one low-reflection elevator door frame is not detected



(**c**) Location of LiDAR where entire high-reflection elevator is detected

Figure 9. Positioning for low- and high-reflection elevator detection.

The experiment for high-reflection elevator recognition was conducted at the central location where the entire elevator structure was detected to verify the elevator gate recognition technique from the significant noise generated by the door frames on both sides of the elevator, as shown in Figure 9c.

Two different gate recognition experiments were conducted for the above two materials, and it was confirmed that the coordinates of the elevator door frame were accurately detected.

3.1.2. H/W Configuration

The RPLIDAR A2, SLAMTEC, was used to verify the elevator recognition technique presented in this study; the specification is shown in Table 1.

Table 1. Specification of LiDAR sensor.

Model	RPLiDAR-A2
Distance range	0.15–6 m
Angular range	0–360 degrees
Angular resolution	0.9 degree
Scan rate	10 Hz
Distance error rate	<1% of the distance

3.2. Experimental Results

This study proposes a noise removal and masking technique, segmentation, and line-segmentation-algorithm-based elevator recognition approach in order to detect the accurate coordinates of elevator door frames as a method for LiDAR-sensor-based elevator recognition.

To verify the proposed method, an experiment was conducted in an environment where an actual elevator was installed, and in which the elevator environment was finished with low- and high-reflective materials, respectively.

The accuracy of the method of low-reflective elevator gate recognition for detecting elevator door frames was verified by conducting an experiment at a location where the LiDAR sensor could recognize the entire elevator gate and at a location where a certain part of the gate was not recognized, respectively.

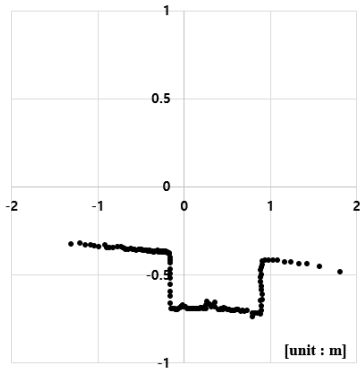
An elevator experiment in which high-reflection material was used verified the accuracy of detecting the elevator door frame coordinates by means of 30 repetitive trials because real-time LiDAR data has an irregular shape due to high surface reflectance.

3.2.1. Results of the Low-Reflective Material Elevator Gate Recognition Experiment

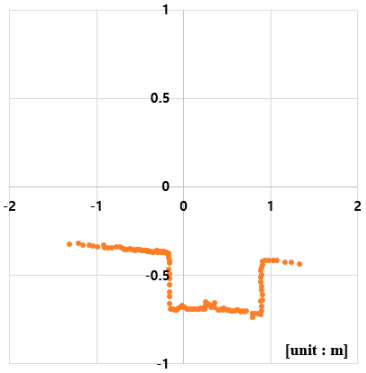
The experiment for elevator recognition with low-reflective materials was conducted in the order of LPF, masking technique, ABD, IEPF, and elevator feature detection algorithms based on the raw data scanned from LiDAR.

Figure 10a shows a raw-data-based point-cloud containing elevator information for low-reflective materials and shows that it has the form of the entire structure of the elevator. Figure 10b shows that one cluster was created through the ABD clustering algorithm from the results of Figure 10a. The results of the IEPF line segment extraction algorithm based on the generated cluster, which are shown in Figure 10c,d, show the elevator door frame coordinates detected through the elevator recognition technique based on the extracted line segments.

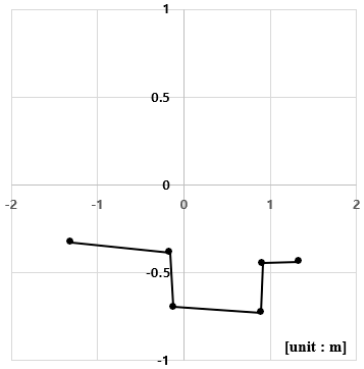
Figure 11 represents the results of the elevator recognition algorithm at the location of the LiDAR sensor where one elevator door frame cannot be detected. Figure 11a is a raw-data-based point-cloud with information from a general elevator. Based on this, it can be seen that a total of two clusters were created as a result of performing the ABD clustering algorithm, which is shown in Figure 11b. The results of performing the IEPF line segment extraction algorithm based on the generated clusters are shown in Figure 11c, and the results for the coordinates detected by performing the elevator recognition technique based on the generated line segments are shown in Figure 11d.



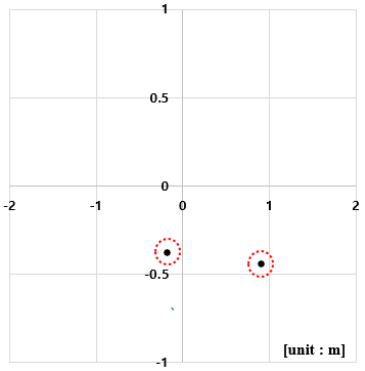
(**a**) LPF and Masking techniques



(**b**) ABD

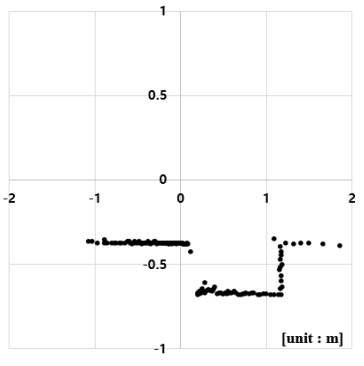


(**c**) IEPF

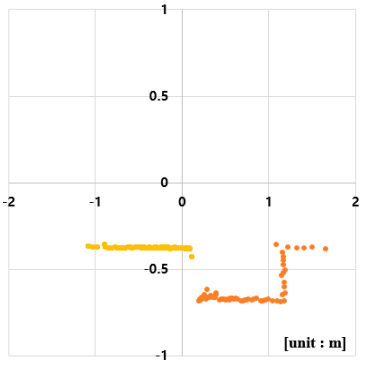


(**d**) Feature extraction

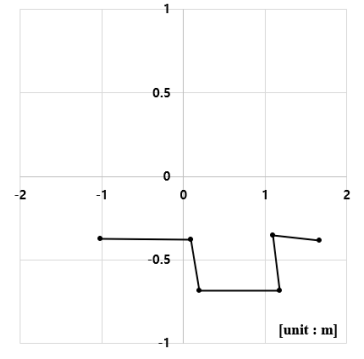
Figure 10. Data pre-processing and detection results of low-reflection elevator where the entire gate is detected.



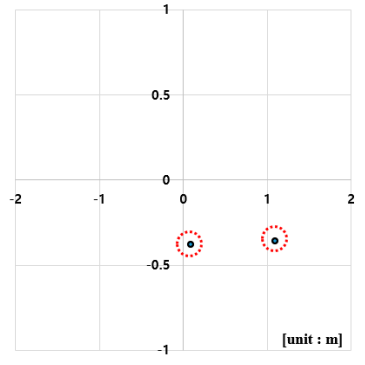
(**a**) LPF and Masking techniques



(**b**) ABD



(**c**) IEPF



(**d**) Feature extraction

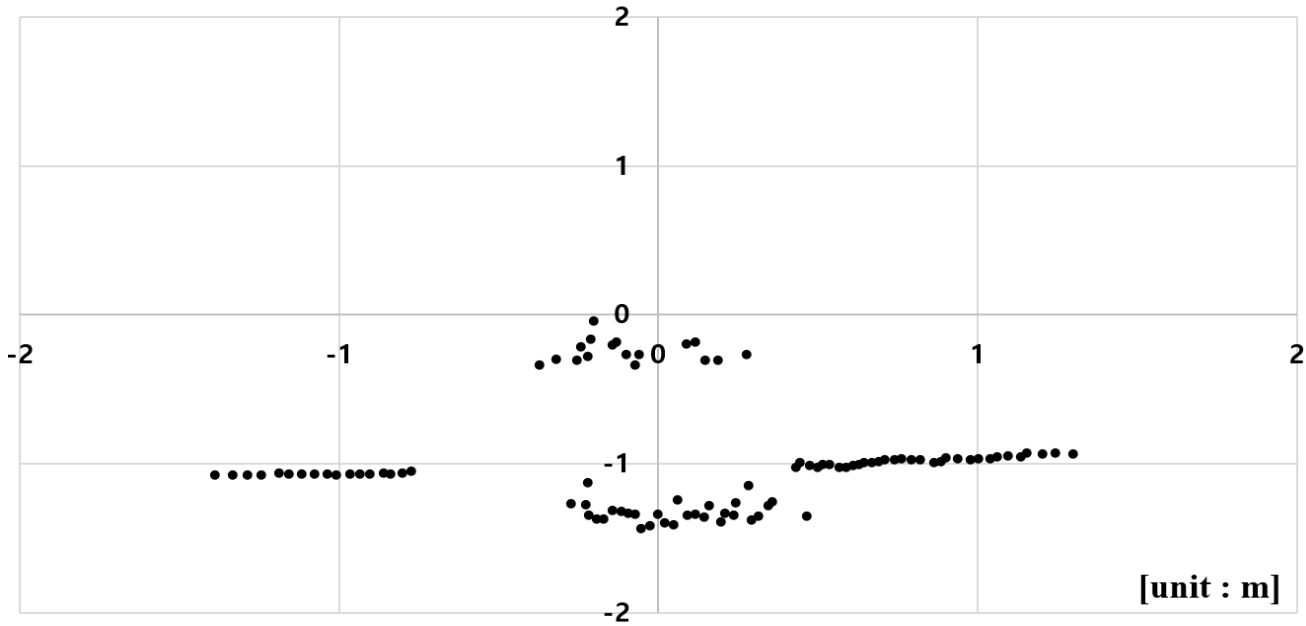
Figure 11. Data pre-processing and detection results of low-reflection elevator where only part of the gate is detected.

The actual elevator width of the experimental environment was 1.08 m, and the distance value of the two coordinates measured at the location where the entire structure of the elevator was recognized was 1.12 m, indicating a maximum error rate of 3.4%. The distance value of the two coordinates measured at the location where one elevator door frame was not detected was 1.14 m, confirming that it had a maximum error rate of 5.3%.

3.2.2. Results of the High-Reflective Material Gate Recognition Experiment

The experiment for elevator recognition with high-reflective materials involved the same procedure as the elevator recognition process for low-reflective materials and was based on the line segments that were carried out in the order of LPF, masking technique, ABD, and IEPF using the raw data.

Figure 12a shows a raw-data-based point-cloud containing the elevator information for high-reflective materials. It can be seen that noise is generated due to the high surface reflectance of the high-reflective elevator materials. Figure 12b is the result of applying LPF and masking techniques from the results of Figure 12a, Figure 12c is the result of creating a total of three clusters through the ABD clustering algorithm, Figure 12d is the result of creating a total of three segments through the IEPF line segment extraction algorithm based on the generated clusters, and Figure 12e represents the elevator door frame coordinates detected through the elevator recognition technique of the high-reflective materials based on the generated line segments.



(a) LiDAR raw data

Figure 12. *Cont.*

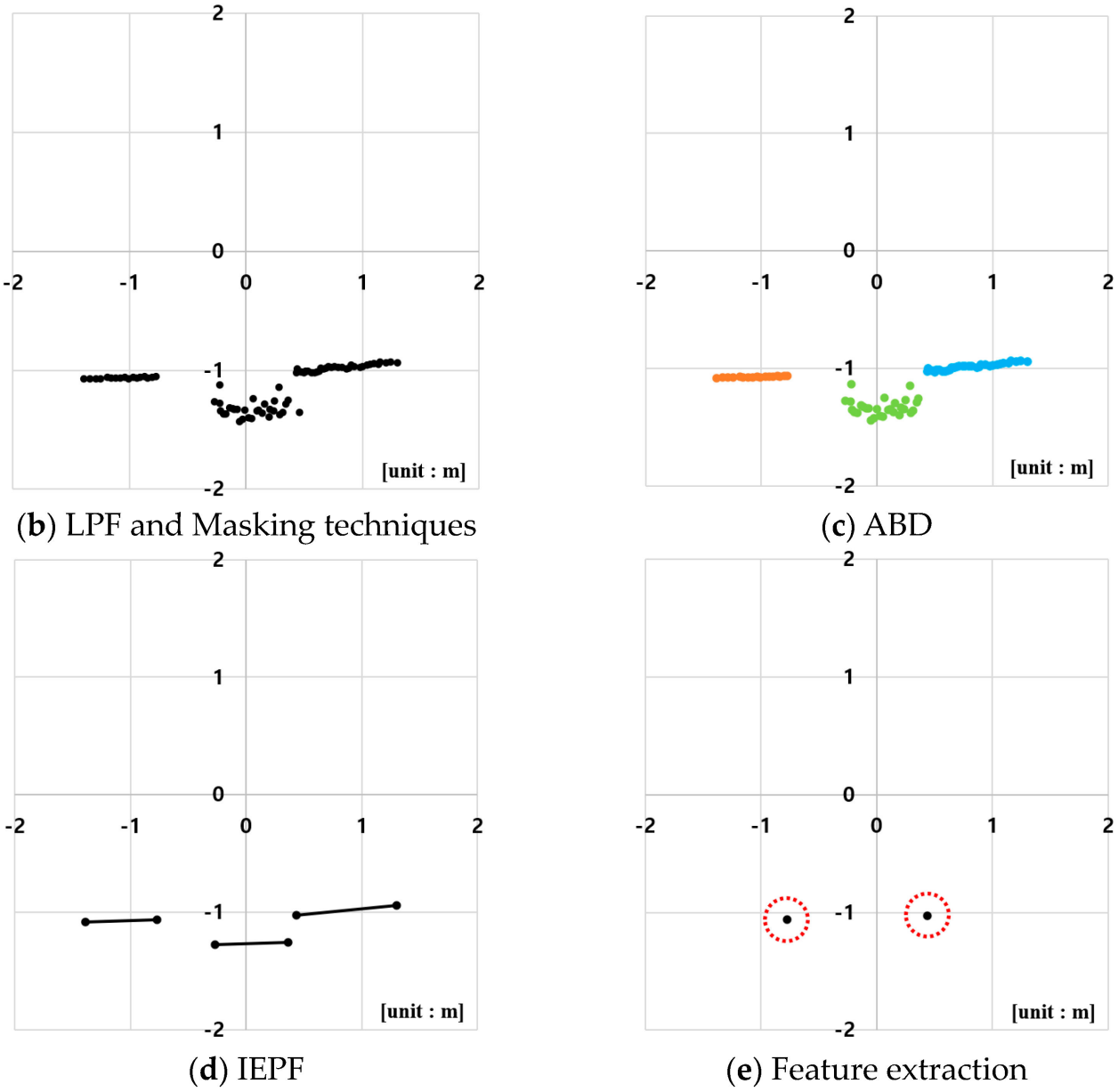


Figure 12. Data pre-processing and detection results of high-reflection elevator.

It was verified that the width of the elevator in the experimental environment was 1.2 m and there was a maximum error rate of 4.847% between the location of the actual elevator door frame and the detected coordinates.

The recognition experiments of the boarding gate of the low- and high-reflection elevator were conducted 30 times each. The accuracy and precision of the recognition algorithm are shown in Table 2. TruePositive (TP) indicates that the algorithm correctly determines the actual elevator type, and FalsePositive (FP) indicates that the algorithm incorrectly determines the actual elevator type.

In a low-reflective elevator environment, the probability TP to be recognized as a low-reflective elevator was 80%, and the probability FP to be determined as a high-reflective elevator was 10%, indicating a maximum precision of 6.11 cm from the actual low-reflective elevator gate width.

Table 2. Experimental results of the elevator detection algorithm.

Number of Experiments, Repeated 30 Times				
Elevator Type	Reflection [%]	Correctness		Precision [cm]
		TruePositive (TP) [%]	FalsePositive (FP) [%]	
Low-reflection elevator	51.3	80.0	10.0	≤6.11
High-reflection elevator	94.2	73.3	6.7	≤5.81

In a high-reflective elevator environment, the probability TP to be recognized as a high-reflective elevator was 73.3%, and the probability FP to be verified as a low-reflective elevator was 6.7%, indicating a maximum precision of 5.81 cm from the actual width of the gate to the high-reflective elevator.

As a result of the experiment, the width of the boarding gate of the low-reflective elevator was 6.11 cm and the width of the boarding gate of the high-reflective elevator was 5.81 cm in terms of the maximum error rate. According to Kim, J., et al. [8], a camera-based elevator recognition study was conducted on elevators with low-reflective and high-reflective materials, and experiments were conducted from 0 to 30 degrees in 10-degree increments from facing the sensor to the front. The detection performance of elevators with low-reflective and high-reflective materials was confirmed with maximum position errors of 4.21 cm and 7.57 cm, respectively.

The threshold value of the masking technique applied in this paper is 2 m, and the distance error rate of the RPLiDAR-A2 used is less than 1% based on the measured distance, resulting in a maximum error rate of 0.02 m or less for the measured data. In addition, considering the minimum door width of 0.8 m for accessible elevators according to the Act on Ensuring Convenience for the Disabled, the Elderly, and Pregnant Women in Korea, and the maximum width of 0.7 m for indoor electric wheelchairs according to the ISO (International Organization for Standardization) standard 7176-5 (Determination of dimensions, mass and manoeuvring space), the results of this experiment confirm that there is no problem in applying the wheelchair active driving technique [28,31].

4. Conclusions

This study proposes a technique for recognizing elevator gates instead of users through LiDAR sensors and elevator recognition algorithms in various elevator environments that require detailed operation. The experiment was conducted in an elevator environment with a low-reflective material and a high-reflective material with a high surface reflectance. For the experiment on the low-reflective elevators examining when the LiDAR sensors detected the entire elevator gate or only a part of the elevator gate, maximum error rates of 3.4% and 5.3% from the actual elevator width were observed, respectively. The elevator recognition experiment made of high-reflective material was repeated 30 times, and the maximum error rate was 4.847% from the actual elevator width.

The low-cost 2D LiDAR-sensing-system-based elevator recognition technique proposed in this paper can be developed as an add-on module for electric wheelchairs, which is expected to solve the difficulties of inexperienced manipulation by wheelchair users at low cost.

However, the technique proposed in this paper may not be suitable for all elevator structures because it cannot be detected with a LiDAR sensor for glass that is permeable. However, it was verified that it can be utilized as a suitable method for the high-reflective surface targeted in this paper. Therefore, in future research, it is necessary to conduct research on glass detection based on a sensor system that fuses LiDAR and ultrasonic sensors to recognize elevators with glass finishes. It is expected that various types of elevator recognition will be possible through research on the technology, thereby contributing to the

elevator boarding and unloading technology that may be employed by wheelchair users with upper limb disabilities.

Author Contributions: Conceptualization and methodology, D.K., S.-H.E. and E.-H.L.; software, D.K.; validation, E.-H.L. and S.-H.E.; formal analysis, D.K. and S.-H.E.; investigation, D.K., S.-H.E. and E.-H.L.; data curation, D.K. and S.-H.E.; writing—original draft preparation, D.K.; writing—review and editing, D.K., S.-H.E. and E.-H.L. All authors have read and agreed to the published version of the manuscript.

Funding: This research received no external funding.

Institutional Review Board Statement: Not applicable.

Informed Consent Statement: Informed consent was obtained from all subjects involved in the study.

Data Availability Statement: The data sets generated during this study are available from the corresponding author on reasonable request.

Acknowledgments: This research was supported by the MSIT (Ministry of Science and ICT), Korea, under the ITRC (Information Technology Research Center) support program (IITP-2023-2018-0-01426) supervised by the IITP (Institute for Information and Communications Technology Planning and Evaluation). This work was supported by the Korea Medical Device Development Fund grant funded by the Korea government (the Ministry of Science and ICT, the Ministry of Trade, Industry and Energy, the Ministry of Health and Welfare, the Ministry of Food and Drug Safety) (Project Number: 1711195455, RS-2020-KD000162). This research was supported by a grant from the Korea Health Technology R&D Project through the Korea Health Industry Development Institute (KHIDI), funded by the Ministry of Health and Welfare, Republic of Korea (HJ20C0058).

Conflicts of Interest: The authors declare no conflict of interest.

References

1. Disability. Available online: https://www.who.int/news-room/fact-sheets/detail/disability-and-health (accessed on 22 October 2023).
2. Shin, H.D.; Ahn, D.H.; Lee, H.A.; Lee, Y.K.; Yang, H.S.; Jo, M.; Lee, S.B.N.; Park, G.S.; Hwang, Y.S.; Sim, W.S.; et al. Customized Power Wheelchair Joysticks Made by Three-Dimensional Printing Technology: A Pilot Study on the Environmental Adaptation Effects for Severe Quadriplegia. *Int. J. Environ. Res. Public Health* **2021**, *18*, 7464. [CrossRef] [PubMed]
3. Boninger, M. *The Manual Wheelchair: What the SCI Consumer Needs to Know*; The University of Washington Model Systems Knowledge Translation Center (UW MSKTC): Seattle, WA, USA, 2011.
4. Boninger, M. *The Power Wheelchair: What the SCI Consumer Needs to Know*; The University of Washington Model Systems Knowledge Translation Center (UW MSKTC): Seattle, WA, USA, 2011.
5. World Health Organization. *Fact Sheet on Wheelchairs*; Technical Report; World Health Organization: Geneva, Switzerland, 2010.
6. Choi, S.W.; Woo, J.H.; Hyun, S.Y.; Jang, J.H.; Choi, W.S. Factors associated with injury severity among users of powered mobility devices. *Clin. Exp. Emerg. Med.* **2021**, *8*, 103–110. [CrossRef] [PubMed]
7. Ohara, E.; Watanabe, T.; Oishi, T.; Aoki, T.; Nishimoto, Y.; Yano, K. Assistance control of wheelchair operation using active cast for the upper limb. In Proceedings of the 2011 IEEE International Conference on Robotics and Automation, Shanghai, China, 9–13 May 2011; pp. 2223–2228.
8. Kim, J.H.; Jung, M.K.; Song, J.B. Getting On and Off an Elevator Safely for a Mobile Robot Using RGB-D Sensors. *J. Korea Robot. Soc.* **2020**, *15*, 55–61. [CrossRef]
9. Kim, E.H.; Bae, S.H.; Kuc, T.Y. Mobile service robot multi-floor navigation using visual detection and recognition of elevator features(ICCAS 2020). In Proceedings of the 20th International Conference on Control, Automation and Systems (ICCAS), Busan, Republic of Korea, 13–16 October 2020; pp. 982–985.
10. Baek, J.Y.; Lee, M.C. A study on detecting elevator entrance door using stereo vision in multi floor environment. In Proceedings of the 2009 ICCAS-SICE, Fukuoka, Japan, 18–21 August 2009; pp. 1370–1373.
11. Ma, S.W.; Cui, X.; Lee, H.H.; Kim, H.R.; Lee, J.H.; Kim, H.I. Robust Elevator Door Recognition using LRF and Camera. *J. Inst. Control Robot. Syst.* **2012**, *18*, 601–607. [CrossRef]
12. Huang, Y.; Wen, Q.; Dong, S. Elevator door state detection method based on semantic segmentation. In Proceedings of the 6th International Symposium on Computer and Information Processing Technology (ISCIPT), Changsha, China, 11–13 June 2021; pp. 109–112.

13. Liang, S.; Niu, D.; Huang, K.; Wu, H.; Ding, L.; Yang, Y. An elevator door blocking behavior recognition method based on two-stage object detection networks. In Proceedings of the 2022 37th Youth Academic Annual Conference of Chinese Association of Automation (YAC), Beijing, China, 19–20 November 2022; pp. 1374–1378.
14. Troniak, D.M.; Sattar, J.; Gupta, A.; Little, J.; Chan, W.P.; Calisgan, E.; Croft, E.A.; Loos, H.F. Charlie rides the elevator—integrating vision, navigation and manipulation towards multi-floor robot locomotion. In Proceedings of the 2013 International Conference on Computer and Robot Vision, Regina, SK, Canada, 28–31 May 2013; pp. 1–8.
15. Amano, R.; Takahashi, K.; Cho, T.; Kobayashi, K.; Watanabe, K.; Kurihara, Y. Development of automatic elevator navigation algorithm for JAUS compliant mobile robot. In Proceedings of the 6th International Conference on Soft Computing and Intelligent Systems, and the 13th International Symposium on Advanced Intelligence Systems, Kobe, Japan, 20–24 November 2012; pp. 1633–1638. Available online: https://ieeexplore.ieee.org/document/6505165 (accessed on 6 November 2023).
16. What Is the Difference Between Front Wheel Drive, Mid Wheel Drive, and Rear Wheel Drive Wheelchairs? Available online: https://hub.permobil.com/blog/difference-between-fwd-mwd-rwd (accessed on 22 October 2023).
17. Front Wheel, Mid Wheel or Rear Wheel Drive. Available online: https://www.electricwheelchairsusa.com/blogs/news/front-wheel-mid-wheel-or-rear-wheel-drive (accessed on 22 October 2023).
18. Unveiling the Precision of Lidar Mapping: How Accurate Is It Really? Available online: https://www.aerial-precision.com/blog/exploring-the-precision-of-lidar-mapping-unveiling-its-accuracy (accessed on 22 October 2023).
19. Korea Legislation Research Institute. Elevator Safety Management Act. Available online: https://elaw.klri.re.kr/kor_service/lawView.do?hseq=62388&lang=ENG (accessed on 22 October 2023).
20. Borges, G.A.; Aldon, M.J. Line Extraction in 2D Range Images for Mobile Robotics. *J. Intell. Robot. Syst.* **2004**, *40*, 267–297. [CrossRef]
21. Duan, J.; Valentyna, A. Road edge detection based on LIDAR laser. In Proceedings of the 2015 International Conference on Control, Automation and Information Sciences (ICCAIS), Changshu, China, 29–31 October 2015; pp. 137–142.
22. Hu, W.; Zhang, K.; Shao, L.; Lin, Q.; Hua, Y.; Qin, J. Clustering Denoising of 2D LiDAR Scanning in Indoor Environment Based on Keyframe Extraction. *Sensors* **2023**, *23*, 18. [CrossRef] [PubMed]
23. Deng, X.S.; Tang, G.; Wang, Q.Y. A novel fast classification filtering algorithm for LiDAR point clouds based on small grid density clustering. *Geod. Geodyn.* **2022**, *13*, 38–49. [CrossRef]
24. Duan, J.; Shi, L.; Yao, J.; Liu, D.; Tian, Q. Obstacle detection research based on four-line laser radar in vehicle. In Proceedings of the 2013 IEEE International Conference on Robotics and Biomimetics (ROBIO), Shenzhen, China, 12–14 December 2013; pp. 2452–2457.
25. Nguyen, V.; Martinelli, A.; Tomatis, N.; Siegwart, R. A comparison of line extraction algorithms using 2D laser rangefinder for indoor mobile robotics. In Proceedings of the 2005 IEEE/RSJ International Conference on Intelligent Robots and Systems 2005, Edmonton, AB, Canada, 2–6 August 2005; pp. 1929–1934.
26. Zhang, L.; Ghosh, B.K. Line segment based map building and localization using 2D laser rangefinder. In Proceedings of the 2000 ICRA. Millennium Conference, IEEE International Conference on Robotics and Automation. Symposia Proceedings, San Francisco, CA, USA, 24–28 April 2000; Volume 3, pp. 2538–2543.
27. Vandorpe, J.; Van Brussel, H.; Xu, H. Exact dynamic map building for a mobile robot using geometrical primitives produced by a 2D range finder. Proceedings of IEEE International Conference on Robotics and Automation, Minneapolis, MN, USA, 22–28 April 1996; Volume 1, pp. 901–908.
28. Korea Legislation Research Institute. Act on The Guarantee of Convenience Promotion of Persons With Disabilities, Senior Citizens, Pregnant Women And Nursing Mothers. Available online: https://elaw.klri.re.kr/kor_service/lawView.do?hseq=57346&lang=ENG (accessed on 22 October 2023).
29. Chen, W.H. Disturbance Observer Based Control for Nonlinear System. *IEEE/ASME Trans. Mechatron.* **2004**, *9*, 706–710. [CrossRef]
30. Chen, W.H.; Yang, J.; Guo, L.; Li, S. Disturbance-Observer-Based Control and Related Methods: An Overview. *IEEE Trans. Ind. Electron.* **2015**, *63*, 1083–1095. [CrossRef]
31. *ISO 7176-5:2008*; Determination of Dimensions, Mass and Manoeuvring Space. International Organization for Standardization: Geneva, Switzerland, 2008. Available online: https://www.iso.org/standard/46429.html (accessed on 22 October 2023).

Disclaimer/Publisher's Note: The statements, opinions and data contained in all publications are solely those of the individual author(s) and contributor(s) and not of MDPI and/or the editor(s). MDPI and/or the editor(s) disclaim responsibility for any injury to people or property resulting from any ideas, methods, instructions or products referred to in the content.